Research, Society and Development, v. 11, n. 6, e14411628873, 2022
(CC BY 4.0) | ISSN 2525-3409 | DOI: http://dx.doi.org/10.33448/rsd-v11i6.28873

Green synthesis with Aloe Vera of $MgAl_2O_4$ substituted by Mn and without calcination treatment

Síntese verde com Aloe Vera do $MgAl_2O_4$ substituído por Mn e sem tratamento de calcinação

Síntesis en verde con Aloe Vera de $MgAl_2O_4$ sustituido por Mn y sin tratamiento de calcinación

Received: 04/05/2022 | Reviewed: 04/12/2022 | Accept: 04/19/2022 | Published: 04/23/2022

Pedro Paulo Linhares Ferreira
ORCID: https://orcid.org/0000-0003-3672-3641
Universidade Federal do Rio Grande do Norte, Brasil
E-mail: pedrolinharesf@gmail.com
Dulce Maria de Araújo Melo
ORCID: https://orcid.org/0000-0001-9845-2360
Universidade Federal do Rio Grande do Norte, Brasil
E-mail: daraujomelo@gmail.com
Rodolfo Luiz Bezerra de Araújo Medeiros
ORCID: https://orcid.org/0000-0002-3072-1250
Universidade Federal do Rio Grande do Norte, Brasil
E-mail: rodolfoluiz.eng@gmail.com
Tomaz Rodrigues de Araújo
ORCID: https://orcid.org/0000-0002-5368-9775
Universidade Federal do Rio Grande do Norte, Brasil
E-mail: tomaz.rdaraujo@bct.ect.ufrn.br
Fernando Velcic Maziviero
ORCID: https://orcid.org/0000-0003-3687-2161
Universidade Federal do Rio Grande do Norte, Brasil
E-mail: velcicf@gmail.com
Ângelo Anderson Silva de Oliveira
ORCID: https://orcid.org/0000-0002-4143-3238
Universidade Federal do Rio Grande do Norte, Brasil
E-mail: angelo_quimica@hotmail.com

Abstract
Magnesium aluminates ($MgAl_2O_4$) with Mn substituting sites A and B were synthesized by the microwave-assisted combustion method applying high power (900 W) using Aloe Vera as a green chelating agent. The study evaluated the effect of the presence of Aloe Vera and the subsequent heat treatment on the structural characteristics of spinel powders by X-ray diffraction (XRD). The effect of heat treatment was evaluated in two ways: with and without calcination. The results showed that the substitutes occurred forming the following phases: $Mg_{0.21}Mn_{2.36}Al_{0.43}O_4$, $Mg_{0.13}Mn_{2.63}Al_{0.25}O_4$, $Mg_{0.31}Mn_{2.06}Al_{0.63}O_4$ substituting site A; and $MgMn_{1.88}Al_{0.13}O_4$ and $MgMn_{1.75}Al_{0.25}O_4$ substituting site B. The presence of Mn and Aloe Vera ions affected the spinel crystal structure. The crystallinity degree is less intense when the magnesium aluminate was substituted by the Mn ion due to the amount of deformations in the crystal system induced by the substituent ion. However, the calcination of the powders increased the crystallinity degree in all scenarios. Furthermore, the substitution caused alteration in the lattice parameters due to the difference between the ionic radius of the substituent and the Mg^{2+} or Al^{3+} ion evidenced in the positions of 2θ. The spinel cubic phase was found in most materials, although the tetrahedral phase was observed in some Mn-substituted structures. The crystallite sizes of the powders were influenced by the presence of phytochemicals present in Aloe Vera. A decrease in crystallite size was observed when the materials were calcined as a result of the gasification of biomolecules from the plant extract. However, these biomolecules help in dissociating precursors, albeit slowly, which prevented crystallite growth. The use of Aloe Vera as a chelating agent proved to be efficient in the synthesis of magnesium aluminate spinels, pointing out the synthesized material as a promising route for the green synthesis field.
Keywords: $MgAl_2O_4$; Aloe vera; Microwave-assisted combustion method; Mn.

Resumo
Aluminatos de magnésio ($MgAl_2O_4$) com Mn substituindo os sítios A e B foram sintetizados através do método de combustão assistida por micro-ondas aplicando alta potência (900 W) utilizando a Aloe Vera como agente quelante verde. O estudo avaliou o efeito da presença da Aloe Vera e do tratamento térmico subsequente nas características estruturais dos pós de espinélios através de difração de raios X (DRX). O efeito do tratamento térmico foi avaliado em duas formas: com e sem calcinação. Os resultados apontaram que as substituições ocorreram formando as seguintes fases $Mg_{0,21}Mn_{2,36}Al_{0,43}O_4$, $Mg_{0,13}Mn_{2,63}Al_{0,25}O_4$, $Mg_{0,31}Mn_{2,06}Al_{0,63}O_4$, substituindo o sítio A. E $MgMn_{1,88}Al_{0,13}O_4$ e

$MgMn_{1,75}Al_{0,25}O_4$, substituindo o sítio B. A presença dos íons Mn e Aloe Vera afetaram a estrutura cristalina do espinélio. O grau de cristalinidade é menos intenso quando o aluminato de magnésio foi substituído pelo íon de Mn, pela quantidade de deformações sistema cristalino induzidas pelo íon substituinte. Entretanto, a calcinação dos pós aumentou o grau de cristalinidade em todos os cenários. Além disso, a substituição causou alteração nos parâmetros de rede em virtude da diferença entre o raio iônico do substituinte e o íon de Mg^{2+} ou Al^{3+}, sendo evidenciado nas posições de 2θ. A fase cúbica do espinélio foi encontrada na maioria dos materiais, embora a fase tetraédrica foi observada em algumas estruturas substituídas com Mn. Os tamanhos dos cristalitos dos pós foram influenciados pela presença de fitoquímicos presentes na Aloe Vera. Foi observado uma diminuição do tamanho do cristalito quando os materiais foram calcinados em decorrência da gaseificação de biomoléculas oriundas do extrato vegetal. Entretanto, estas biomoléculas ajudam na dissociação dos precursores, embora seja de forma lenta, o que impediu o crescimento do cristalito. O uso de Aloe Vera como agente quelante se mostrou eficiente na síntese dos espinélios de aluminato de magnésio, apontando o material sintetizado como uma via promissora para o campo da síntese verde.
Palavras-chave: $MgAl_2O_4$; Aloe vera; Combustão por microondas; Mn.

Resumen
Los aluminatos de magnesio (MgAl2O4) con Mn reemplazando los sitios A y B fueron sintetizados por el método de combustión asistida por microondas aplicando alta potencia (900 W) utilizando Aloe Vera como agente quelante verde. El estudio evaluó el efecto de la presencia de Aloe Vera y el posterior tratamiento térmico sobre las características estructurales de los polvos de espinela por difracción de rayos X (XRD). El efecto del tratamiento térmico se evaluó de dos formas: con y sin calcinación. Los resultados mostraron que las sustituciones ocurrieron formando las siguientes fases $Mg_{0,21}Mn_{2,36}Al_{0,43}O_4$, $Mg_{0,13}Mn_{2,63}Al_{0,25}O_4$, $Mg_{0,31}Mn_{2,06}Al_{0,63}O_4$, reemplazando el sitio A. Y $MgMn_{1,88}Al_{0,13}O_4$ y $MgMn_{1,75}Al_{0,25}O_4$, reemplazando el sitio B. La presencia de iones Mn y Aloe Vera afectó la estructura cristalina de la espinela. El grado de cristalinidad es menos intenso cuando el aluminato de magnesio fue reemplazado por el ion Mn, debido a la cantidad de deformaciones en el sistema cristalino inducidas por el ion sustituyente. Sin embargo, la calcinación de los polvos aumentó el grado de cristalinidad en todos los escenarios. Además, la sustitución provocó alteración en los parámetros de la red debido a la diferencia entre el radio iónico del sustituyente y el ion de Mg^2 o Al^3, evidenciándose en las posiciones de 2θ. La fase cúbica de la espinela se encontró en la mayoría de los materiales, aunque la fase tetraédrica se observó en algunas estructuras sustituidas con Mn. Los tamaños de cristalitos de los polvos fueron influenciados por la presencia de fitoquímicos presentes en el Aloe Vera. Se observó una disminución en el tamaño de los cristalitos cuando los materiales fueron calcinados como resultado de la gasificación de las biomoléculas del extracto vegetal. Sin embargo, estas biomoléculas ayudan en la disociación de precursores, aunque lentamente, lo que impidió el crecimiento de cristalitos. El uso de Aloe Vera como agente quelante demostró ser eficiente en la síntesis de espinelas de aluminato de magnesio, señalando el material sintetizado como una ruta prometedora para el campo de la síntesis verde.
Palabras clave: MgAl2O4; Aloe vera; Combustión de microondas; Mn.

1. Introduction

Magnesium aluminate spinel ($MgAl_2O_4$) has a peculiar combination of interesting properties which gives it a prominent position in the research of the scientific community, such as high melting point (2135°C), good mechanical strength at both room temperature (135-216 MPa), and at more severe temperatures (120-205Mpa at 1300°C), relatively low density (3.48 $g.cm^{-3}$), high resistance to chemical attack, low dielectric constant, excellent optical properties, good catalytic properties and low thermal expansion (Ganesh, 2013). In addition, $MgAl_2O_4$ has low acidity, satisfactory hydrothermal stability, good interaction with the active species (Govindarajan & Roy, 2020), expressive chemical inertia, high mechanical strength and high thermal stability (Yu et al., 2021). Therefore, magnesium aluminate has been widely used in industrial applications (Alvar et al., 2010) as catalysts or catalyst supports in environmental catalysis fields (Guo et al., 2004). The variety of properties of $MgAl_2O_4$ is maximized due to its structural complexity, so it is intuitive to consider that its processing plays a very important role. Given this, there are numerous synthesis routes present in the literature. Among them, the solid-solid reaction (Khorramirad et al., 2018), (Rahmat et al., 2018), hydrothermal synthesis (Jung et al., 2018), (R. Li et al., 2020), SOL-GEL (Sanjabi & Obeydavi, 2015), (Boroujerdnia & Obeydavi, 2016), the Pechini method (Golyeva et al., 2018), (Golyeva et al., 2020) and microwave-assisted combustion (Baghbanzadeh et al., 2011), (Ganesh et al., 2005), (Medeiros et al., 2016), (Yousefi et al., 2018); the latter stands out among the cited syntheses because of its numerous advantages such as short synthesis time, low cost, simplicity and more uniform, more crystalline and higher purity particulate production. In addition, the microwave-assisted combustion method requires less

external energy (Carvalho et al., 2018). In addition to the advantages already mentioned, microwave heating in chemical processes has another great potential, as it allows for more uniform temperature distribution in both time and space, high heat and mass transfer in microstructured chemical reactors and higher reaction rates (Sturm et al., 2010).

The spinel is a structure which enables several modifications through other elements or by changing the reaction medium in the synthesis. Thus, combining these variables can produce unique properties which open up possibilities for diverse applications. The substitution of ions from both site A and site B can change the structural and physicochemical characteristics, as well as the electrical properties. The literature points out many metal doping forms in $MgAl_2O_4$ to evaluate its structure and applications (Alam et al., 2021), (Katheria et al., 2019), (Liu et al., 2021), (Sun et al., 2021), however, little is known about the doping of Mn in magnesium aluminate. A study investigated the mixed doping of Mn and Fe in MgAl2O4, CeO2, ZrO2 and Y2O3-ZrO2 for application and feasibility Chemical Looping Combustion (CLC) and Chemical Looping with Oxygen Uncoupling (Azimi et al., 2014). In another research, the variation of the photoluminescence composition of Mn-doped magnesium aluminate spinel was evaluated (Sakuma et al., 2014). Despite the records in the scientific community regarding manganese ion doping in the spinel structure, the combined effects of substitution of sites A and B with the presence of natural chelating agents, such as Aloe Vera extract, and without the need for calcination have not yet been studied.

The extract of Aloe barbadensis Mill, which is part of the Liliaceal family and popularly known as Aloe Vera, is normally used for cosmetic and medicinal purposes (R H Davis, M G Leitner, 1988), however, the plant still has soothing, immunomodulatory, protective properties against ultraviolet rays (Routray et al., 2019), promoting wound and burn healing (Grindlay & Reynolds, 1986), and anti-inflammatory action (Reynolds & Dweck, 1999). This plant extract has more than 75 phytochemical compounds, which are arranged in vitamins (vitamin A, C, E and B12), enzymes (catalase and peroxidase), minerals such as calcium, copper and selenium, anthroquinones, fatty acids, hormones, in addition to of salicylic acid, lignin, saponins (Sánchez et al., 2020), alkaloids, phenols, flavonoids and terpenes (Kumar et al., 2017). These structural characteristics of Aloe Vera make the extract promising for the synthesis of metal nanoparticles and metal oxides (Modanlou Juibari & Eslami, 2019), (Chandran et al., 2006), (LAOKULa et al., 2008). This form of synthesis using Aloe Vera as a biomaterial is more ecological, safe and economical compared to more conventional chemical methods (Modanlou Juibari & Eslami, 2019). This feature in the synthesis of biomolecules with the plant extract is also due to its ability to coordinate with metal ions, since these ions are packaged in helical amylose, which casually leads to the formation of metal oxide (Ragupathi et al., 2014).

Therefore, the objective of this work is to prepare the $MgAl_2O_4$ spinel substituting site A and site B by the Mn^{2+} ion ($Mg_{0.5}Mn_{0.5}Al_2O_4$ and $MgMn_{0.5}Al_{1.5}O_4$, respectively) and to correlate the effect of the presence of Aloe Vera extract as a chelating agent together with heat treatment.

2. Method

2.1 Materials

First, the following were utilized: $Mn(NO_3)_2.4H_2O$ (98%, 251.01 g/mol, Sigma Aldrich); $Al(NO_3)_3.9H_2O$ (98%, 275.13 g/mol, (Sigma Aldrich); $Mg(NO_3)_2.6H_2O$ (98%, 256.41 g/mol, ISOFAR); CH_4NO_2 (99%, 60.06 g/mol, VETEC), distilled water and an aloe vera solution as the chelating agent.

2.2 Preparation of Aloe Vera Aqueous Extract

Freshly harvested leaves of Aloe barbadensis Mill (Aloe Vera) were washed with tap water. Then, the skin was removed by means of a fine cut to preserve the internal gel, which was then sieved in a simple commercial sieve. After the resulting gelatinous extract 100 mL of distilled water was added and stirred for 30 minutes at room temperature forming an aqueous extract. Finally, the extract obtained was stored in a conventional refrigerator at a temperature of approximately 4°C until further

use.

2.3 Support synthesis

First, the reagents were solubilized in 20 ml of distilled water or Aloe Vera, with 50% excess of urea, and then the obtained solution was placed in a microwave oven using a power of 900 W to synthesize the pure $MgAl_2O_4$ using water or Aloe Vera as the green chelating agent. The combustion reaction was observed within 3-4 min of exposure to microwaves. Part of the powders obtained were calcined at 900°C for 3 hours at a rate of 10°C.min^{-1}. The processes for doping with Mn were the same, however, the precursor salt of the Mn^{2+} ion was additionally solubilized in such a way that the ion was stoichiometrically substituted for site A (Mg^{2+}) and site B (Al^{3+}) of magnesium aluminate.

The obtained powders were generally designated as follows: pure non-calcined magnesium aluminate (MAO), calcined (MAO900), non-calcined using Aloe Vera as chelating agent (MAO-AV), and calcined using Aloe Vera as chelating agent (MAO-AV900). The following nomenclature was used for supports doped at site A with the Mn^{2+} ion: non-calcined doped magnesium aluminate (Mn-SA), calcined doped magnesium aluminate (Mn-SA900), non-calcined doped magnesium aluminate with Aloe Vera as chelating agent (Mn-SAAV), and calcined doped magnesium aluminate with Aloe Vera as chelating agent (Mn-SAAV900). Finally, the following nomenclature was used for the supports doped at site B with the Mn^{2+} ion: non-calcined doped magnesium aluminate (Mn-SB), calcined doped magnesium aluminate (Mn-SB900), non-calcined doped magnesium aluminate with Aloe Vera used as chelating agent (Mn-SBAV), and calcined doped magnesium alumina with Aloe Vera used as chelating agent (Mn-SBAV900).

2.4 Characterization

The samples were analyzed by an XRD 7000 diffractometer (SHIMADZU) with a CuKα radiation source (λ = 1.5406 Å), 30 kV voltage and 30 mA current, operating with 2θ scan (10 to 80°); speed of 2°.min^{-1} and step 0.02°. The crystallite size (Dhkl) was calculated by the Scherrer equation (Eq. 01):

$$D(hkl) = \frac{0.9 \times \lambda}{\beta \cos\theta}$$

In which: λ is the wavelength of the X-ray (1.5406 Å); β is the full width half-maximum measure (FWHM) of the diffraction peak and θ is the Bragg angle. $MgAl_2O_4$ measurements were taken at the main peak (2θ = 36.9°; flat (311)) using Al_2O_3 (2θ = 43.32°; (113)) as a standard. The crystalline system for each phase was determined through refinement using the Rietveld method, supported by the Maud version 2.76 software program (MAUD - Materials Analysis Using Diffraction, n.d.).

3. Results and Discussion

Figure 01a shows the X-ray diffractograms of magnesium aluminate in its pure state compared to the same material with Mn^{2+} doped at site A, using or not using Aloe Vera as a chelating agent, with or without heat treatment at 900°C, and with JCPDS letter No. 01-075-1796 as standard. The diffractograms show the main peaks of pure $MgAl_2O_4$ which are present at 2θ = 31.29°; 36.87°; 44.83°; corresponding to planes (220), (311), (400), respectively. The crystallographic profile is in agreement with magnesium aluminate spinel with a cubic structure, corroborating other studies (Alhaji et al., 2019), (Takebuchi et al., 2020), (Q. Y. Chen et al., 2010). In addition, according to the crystallographic profile presented, there was no formation of secondary phases. The materials that were subjected to calcination showed more intense peaks, indicating an increase in crystal nucleation (Ewais et al., 2017). According to the data presented, the use of Aloe Vera as a chelating agent proved to be efficient for synthesizing magnesium aluminate.

The XRD patterns of magnesium aluminates doped at site A with the Mn ion using or not using Aloe Vera as a chelating agent and with or without heat treatment at 900°C are also shown in Figure 01a. The peaks and intensities of the synthesized materials are present at 2θ = 31.08°, 36.63°, 44.53°, corresponding to the planes (220), (311), (400), respectively, indicating that the spinel phase was formed in all samples which were doped (Silva et al., 2017). The absence of peaks referring to the oxides Al_2O_3, MgO, Mn_3O_4, Mn_2O_3 or MnO suggests that secondary phases did not form after the synthesis. This may be related to the fact that the substitution at sites A and B by Mn remained within the solubility limit of the system (Silva et al., 2017).

In comparison with standard magnesium aluminate, it was observed that the peaks underwent a slight shift to the left (Figure 1b), indicating that the lattice constant slightly increases with doping with the Mn ion (Jouini et al., 2006), obeying Vegard's law (Callister, 2007). The increase in the lattice parameter may also be associated with the ionic radius size of the manganese ion (0.80 Å) and Mg^{2+} (0.65 Å) (Callister, 2007). Furthermore, the same XRD patterns of powders doped with manganese ion showed that the Aloe Vera used was effective for spinel formation as well as its substitution. Furthermore, in the regions of the same peaks, the new phases $Mg_{0.21}Mn_{2.36}Al_{0.43}O_4$ and $Mg_{0.13}Mn_{2.63}Al_{0.25}O_4$, whose charts are JCPDS No. 01-075-0525 and JCPDS No. 01-075-0526, respectively, along with the magnesium aluminate phase were identified, except for the peak 2θ = 55.31°, where $MgAl_2O_4$ is not identified. As in the standard powder, the materials that underwent heat treatment had higher peak intensity, suggesting greater crystallinity. Furthermore, all aluminate peaks doped at site A with manganese ion showed a less intense profile compared to the standard. The study indicates that this behavior, which promotes lower intensity peaks, is due to the presence of the dopant in the lattice, causing uniform deformation in the structure resulting from the difference between the atomic radii of the elements involved. This data is also in agreement with other authors (Silva et al., 2017), (Xie et al., 2021).

A decrease of 2θ (peak shift to the left) was observed for all doped samples (Figure 1b). This behavior is expected, as it indicates the substitution of the manganese ion in the magnesium aluminate structure, in addition to pointing out the relevance of the substitution in the $MgAl_2O_4$ structure (Xiao et al., 2012). This occurs since there is a widening of the lattice due to the ionic size difference, which for Mg^{2+} = 0.65 Å and for Mn^{2+} = 0.81Å (Shahid et al., 2020), (Yıldırım et al., 2013). It is also estimated that there was an increased dislocation density for the samples which obtained a displacement of 2θ due to the dopant, thus causing greater resistance to the material flow, causing greater shear stress for the discordant movement (Shivananjaiah et al., 2020). Table 1 highlights the difference in the lattice parameter of the synthesized samples, in addition to the symmetries.

Figura 1. (a) Diffractograms of $MgAl_2O_4$ samples with doped Mn at site A compared to pure $MgAl_2O_4$. (b) Displacement of the main peak of $MgAl_2O_4$ at position 2θ = 36.87° of those substituted by Mn^{2+} in site A.

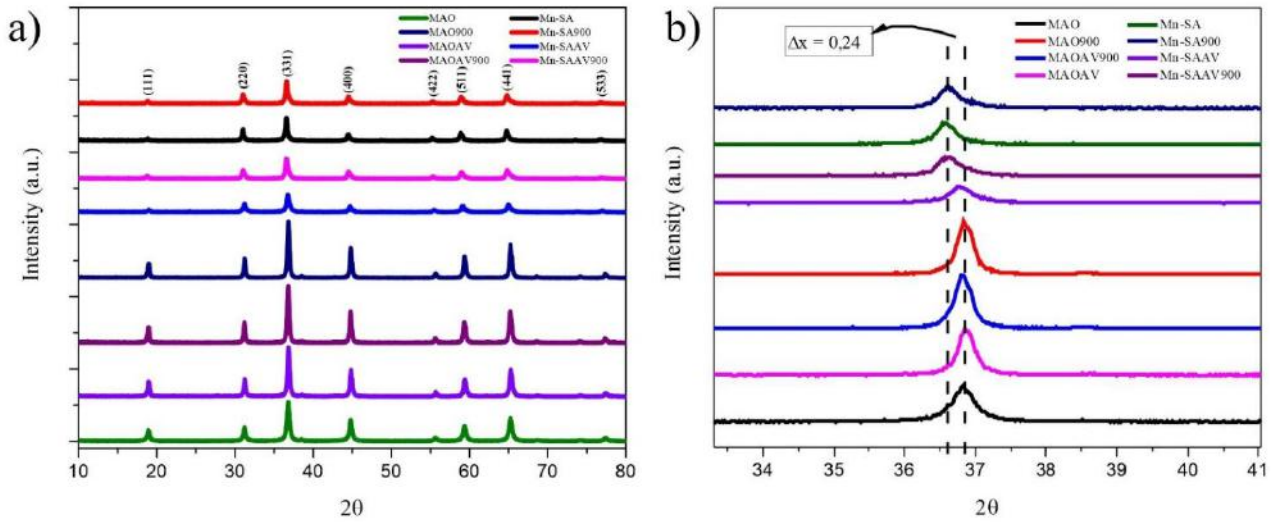

Source: Research data (Ferreira et al., 2022).

Figure 2 shows the crystallographic profile of $MgAl_2O_4$ with the Mn ion doped at site B, using or not using Aloe Vera as a chelating agent and with or without heat treatment at 900°C. XRD patterns show similar peaks and intensities to standard magnesium aluminate, and may indicate spinel phase formation in all samples. Two compounds were identified $MgMn_{1.88}Al_{0.13}O_4$ and $MgMn_{1.75}Al_{0.25}O_4$ (JCPDS no. 01-075-0527e 01-075-0528, respectively), pointing out that the manganese ion was doped at site B of the magnesium aluminate structure. However, $MgMn_{1.75}Al_{0.25}O_4$ only appears at 2θ = 18.61°. The displacement of 2θ was smaller for the Mn-SAAV, Mn-SB and Mn-SBAV materials (Figure 2b). The study suggests that this is due to the preference regarding the structural stability of the manganese ion in tetrahedral sites (Figure 8), causing this retreat to be a little less accentuated (X. Y. Chen et al., 2009). Another study points out that this same event highlights the peak widening caused by tetragonal symmetry (Qiu et al., 2018).

Figure 2. Diffractograms of $MgAl_2O_4$ samples with doped Mn at site B compared to pure $MgAl_2O_4$. (b) Displacement of the main peak of $MgAl_2O_4$ at position 2θ = 36.87° of those substituted by Mn^{2+} at site B.

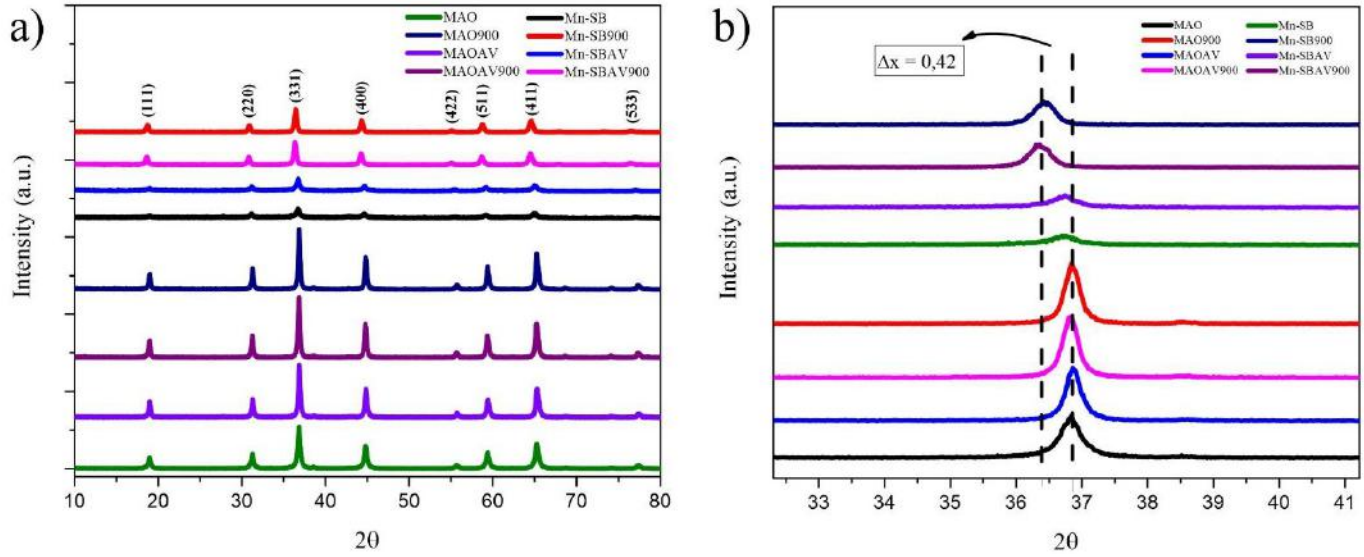

Source: Research data (Ferreira et al., 2022).

Table 1. Lattice parameters and symmetry of $MgAl_2O_4$ samples with doped Mn at site A and B.

Material	Symmetry	Lattice parameters
MAO	Cubic	a: 8.08
MAO900	Cubic	
MAOAV	Cubic	
MAOAV900	Cubic	
Mn-SA	Tetragonal Tetragonal Cubic	a: 5.82 / c: 8.19 a: 5.76 / c: 9.29 a: 8.13
Mn-SA900	Tetragonal Tetragonal Cubic	a: 7.05 / c: 4.45 a: 5.32 / c: 9.34 8.13
Mn-SAAV	Tetragonal Tetragonal Cubic	a: 5.5 / c: 8.6 a: 5.8 / c: 9.9 a: 8.13
Mn-SAAV900	Tetragonal Tetragonal Cubic	a: 38.6 / c: 21.9 a: 5.76 / c: 9.61 8.12
Mn-SB	Tetragonal Cubic	a: 5.83 / c: 8.29 8.12
Mn-SB900	Cubic Tetragonal Cubic	8.15 a: 5.72 / c: 8.91 8.21
Mn-SBAV	Cubic Tetragonal Cubic	8.07 a: 5.04 / c: 6.41 8.11
Mn-SBAV900	Cubic Tetragonal Cubic	8.15 a: 5.76 / c: 8.86 8.22

Source: Research data (Ferreira et al., 2022)

Figure 03 shows the particle size of the powders obtained from pure magnesium aluminates: MAO, MAO900, MAOAV, MAOAV900, as well as the Mn-doped supports at sites A and B: Mn-SA, Mn-SA900, Mn-SAAV, Mn-SAAV900, Mn-SB, Mn-SB900, Mn-SBAV and Mn-SBAV900.

Magnesium aluminate without calcination (MAO) presented the smallest particle size compared to the other samples and syntheses. MAO900 showed the largest particle size compared to MAO, indicating that the heat treatment was decisive for this increase. The use of Aloe Vera in the synthesis of MAOAV and MAOAV900 caused a different behavior. MAOAV has a larger particle size compared to the same calcined sample (MAOAV900) due to the presence of Aloe Vera biomolecules which change the particle size (Selvarajan & Mohanasrinivasan, 2013). The MAOAV sample still has a larger crystallite size because of the polymeric complexes that Aloe Vera has chelated in its structure. When the material is subjected to calcination (MAOAV900), the biomolecules decompose into gaseous products present at high temperatures (Thongam & Chaturvedi, 2021).

For the supports doped with manganese in site A: Mn-SA, Mn-SA900, Mn-SAAV, Mn-SAAV900, Figure 04 shows that the Mn-SA obtained a larger crystallite size compared to the other samples doped in site A. The particle size for Mn-SA900 is smaller than Mn-SA, but larger than Mn-SAAV and Mn-SAAV900. Calcination of the Mn-doped material at site A resulted in a decrease in crystallite size. This behavior is probably due to the presence of nitrates still trapped in the Mn-SA structure. In addition, there is a decrease in oxygen vacancies when the material is calcined at 900°C (Mn-SA900), which interferes with the crystallite size (Milani et al., 2021). The presence of Aloe Vera also influences in order to mask the crystallite size due to existing

phytochemicals in the plant extract, such as phenolics, terpenoids, vitamins, alkaloids, glycosides and flavonoids (Chandrababu et al., 2020), (Mahendiran et al., 2017), (Nasrollahzadeh et al., 2020). These phytochemicals act as natural surfactants and inhibit crystallite growth (Thongam & Chaturvedi, 2021), (Rasli et al., 2020). The same study points out that the dissociation of metallic precursors from the ions involved, which is activated by the biomolecules present in the Aloe Vera extract, is slow and has a weak reduction capacity, preventing nucleation and subsequent non-growth of the crystal.

Describing a reaction mechanism for the synthesis of spinels with Aloe Vera is complex due to the non-crystalline biochemical impurities present in the plant extract. However, a sustainable reaction mechanism for crystal formation is the interaction of metal ions that bind with biomolecules through functional groups and π electrons by ionic bonds or van der Waals forces. Consequently, the crystal size of spinels depends on the concentration of plant extracts and reducing capacity (Ragupathi et al., 2014), (Sangeetha et al., 2011), since the biomolecular complexes cap the metallic particles (Venkateswarlu & Yoon, 2015). The complex structures present in Aloe Vera undergo hydrolysis and subsequent micellization surrounding the metal ions, forming the particle. These surrounding biomolecules act as a natural surfactant, inhibiting nanoparticle agglomeration (Thongam & Chaturvedi, 2021) and interfering with crystal size. Figure 03 below shows an example of a phytochemical (polyphenol) encapsulating the metal ion involved in the reaction forming a biomolecular complex.

Figure 3. Formation of a biomolecular phytochemical complex (polyphenol)-metal ion.

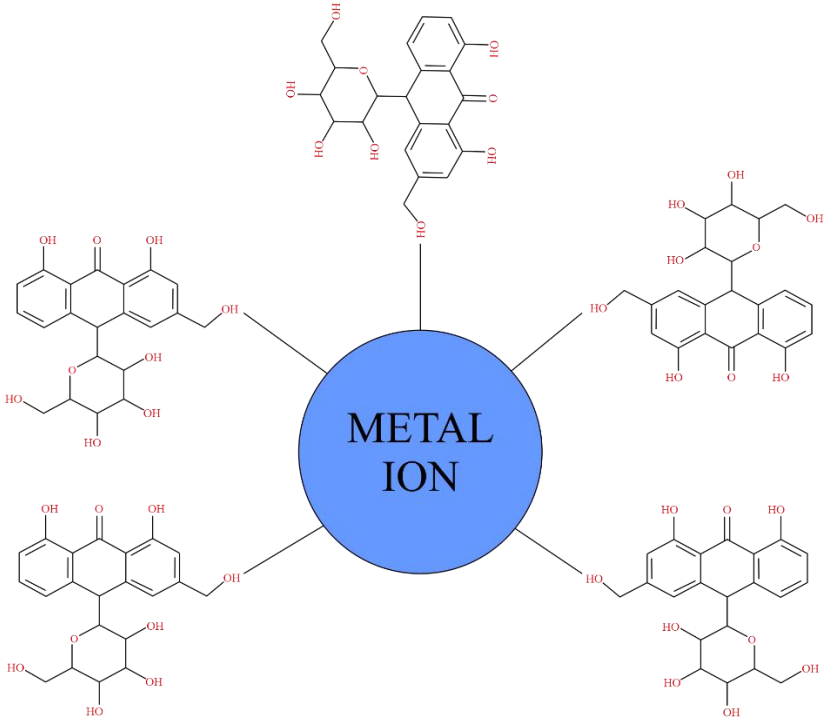

Source: adapted from (Thongam & Chaturvedi, 2021).

The spinels doped with manganese at site B: Mn-SB, Mn-SB900, Mn-SBAV and Mn-SBAV900 presented a similar profile to that found for the magnesium aluminate samples with the manganese ion doped at site A regarding particle size, except for Mn-SB, which showed a much larger particle size, even among all samples and in all conditions and syntheses. In addition to the reasons cited for the samples doped at site A, this is due to the need for structural stability of the cationic ions involved to maintain the charge balance (X. Y. Chen et al., 2009), as well as the presence of only two phases for Mn-SB compared to the other samples with doping at site B (Table 02), which gives a larger crystallite size. In summary, the more phases the material has, the smaller the crystallite size (Wenisch et al., 2016) due to a structural disorder (Saha et al., 2013). The powder calcination (Mn-SB900) resulted in a sudden decrease in particle size as more crystalline structures appeared (Wenisch et al., 2016).

However, when the powder is synthesized with Aloe Vera, the crystallographic behavior is different from that observed previously. Mn-SBAV has a smaller particle size when the same material is calcined (Mn-SBAV900), now influenced by the decrease in phase percentage.

Figure 3. Crystallite size of pure $MgAl_2O_4$ and doped Mn samples at sites A and B.

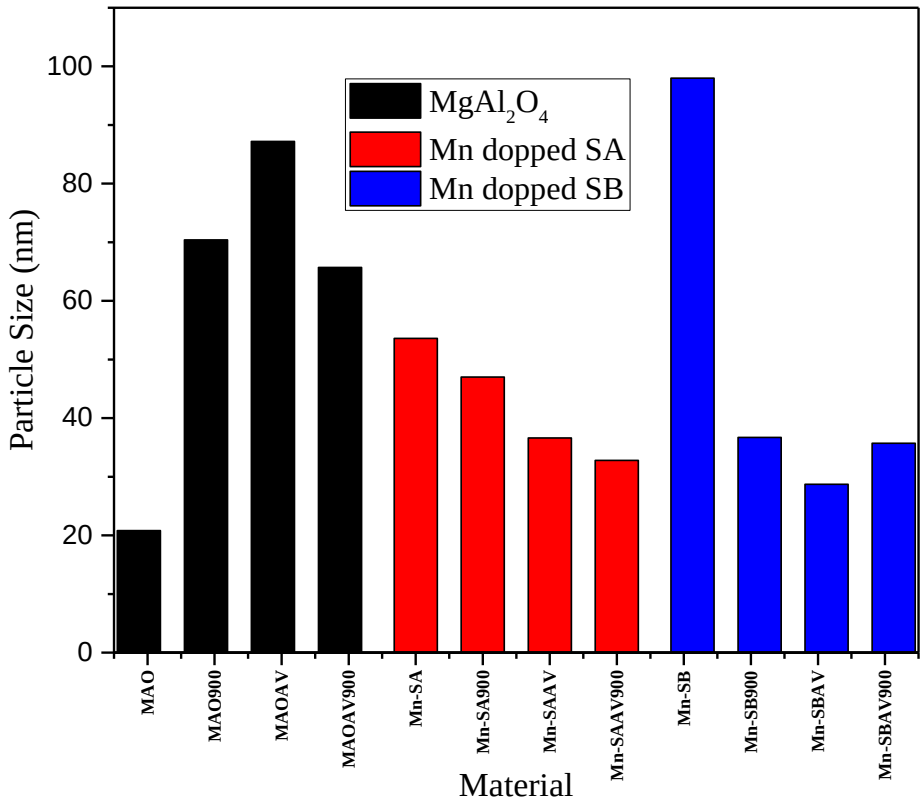

Source: Research data (Ferreira et al., 2022)

Figure 4 shows the crystallinity degree of the synthesized supports. A promotion in the crystallinity degree of the material was observed when the heat treatment is applied for pure magnesium aluminate with Aloe Vera used as a chelating agent or not, and with or without calcination (MAO, MAO900, MAOAV and MAOAV900), corroborating with other studies (Alhaji et al., 2019), (Hao et al., 2021), (Milani et al., 2021), (Figueredo et al., 2017). Furthermore, the increase in the intensity of the peaks observed in the crystallographic profiles may occur as a result of the crystallinity degree which increases with the increase in the calcination temperature (Nantharak et al., 2017), (G. Li et al., 2007), (Hao et al., 2021). The same behavior was observed for the supports doped with manganese at site A and B under all synthesis conditions. However, the crystallinity degree obtained a smaller difference between calcined and non-calcined for the supports doped with manganese ion at site A. The study points out that this fact occurs due to the presence of the manganese ion in the magnesium aluminate structure, hindering a more intense crystallinity due to the amount of deformations induced by the dopant (Chopade et al., 2018). The supports doped with manganese in site B which were calcined had the greatest difference in crystallinity degree when compared to the same supports (SB) which were not calcined; this is due to the lack of structural stability of the manganese ion in the substitution at site B in the interstices of $MgAl_2O_4$, then forming larger non-doped specimens of magnesium aluminate, since manganese ions preferentially occupy tetrahedral sites (Shahid et al., 2020), while there was no favoring the formation of tetrahedral symmetry

in site B. This is due to the adopted heat treatment, which strongly affects the surface structure of the spinel. The material becomes more chemically and thermally stable when calcined (Nascimento et al., 2020), being induced to its most stable state.

Figure 4. Crystallinity degree of samples of pure $MgAl_2O_4$ and doped Mn at sites A and B.

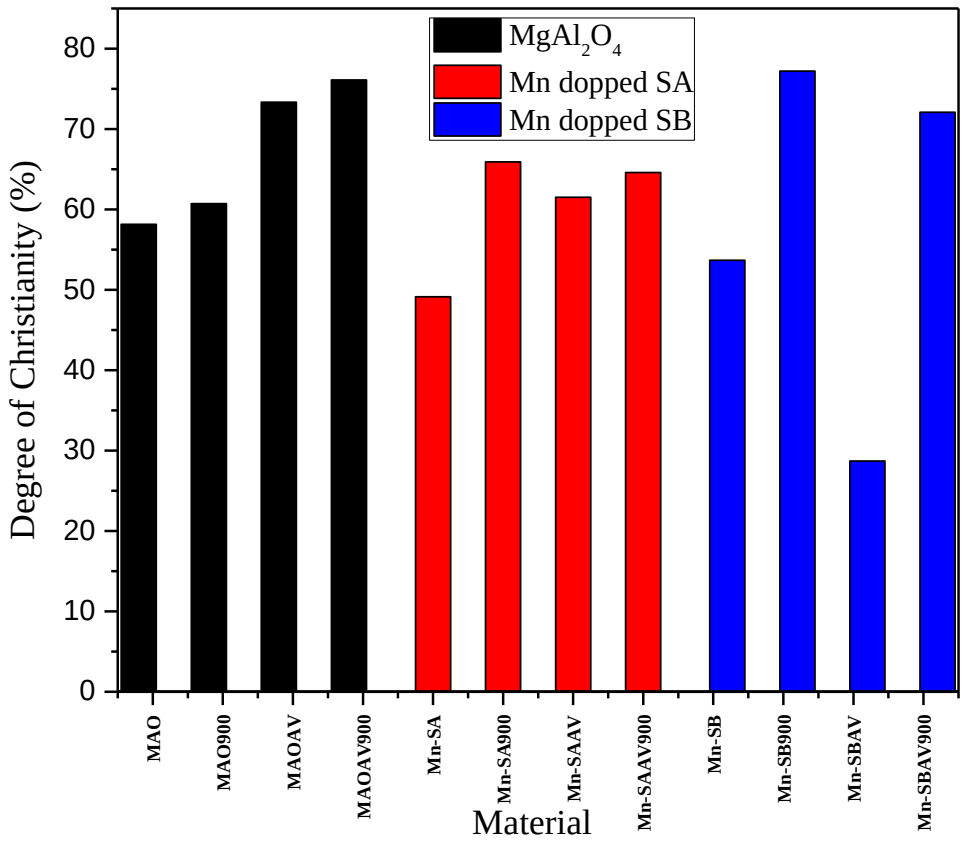

Source: Research data (Ferreira et al., 2021)

Figure 5 shows the percentage as to the concentration of the synthesized supports. The pure magnesium aluminate samples showed 100% of the $MgAl_2O_4$ phase with cubic symmetry. The phase concentration profile changes when magnesium aluminate is doped at site A. There is a predominance of the $Mg_{0.33}Mn_{2.06}Al_{0.63}O_4$ phase for Mn-SA with 99.32% with cubic symmetry. Only traces of $Mg_{0.13}Mn_{2.63}Al_{0.25}O_4$ (0.40%) $Mg_{0.21}Mn_{2.36}Al_{0.43}O_4$ (0.27%), which have tetragonal symmetry, were observed. This same majority pattern of the $Mg_{0.33}Mn_{2.06}Al_{0.63}O_4$ phase is observed in the other supports with manganese doped at site A: Mn-SA900, Mn-SAAV and Mn-SAAV900, however with slightly different percentages.

The predominant phase concentration for manganese doped at site B of magnesium aluminate (Mn-SB) is 62.61% corresponding to $MgMn_{1.75}Al_{0.25}O_4$ with cubic symmetry, versus 37.39% of $MgMn_{1.88}Al_{0.13}O_4$ with tetragonal symmetry. While there was 97% concentration of the $MgAl_2O_4$ phase with cubic symmetry for Mn-SB900, versus 2.33% concentration of the $MgMn_{1.75}Al_{0.25}O_4$ phase and 0.26% of the $MgMn_{1.88}Al_{0.13}O_4$ phase, both with cubic and tetragonal symmetry, respectively. No significant changes in phase concentration are observed when magnesium aluminate powders are synthesized with Aloe Vera. A small trace of $MgAl_2O_4$ phase, corresponding to 0.06% (cubic symmetry) of the phase concentration was found for Mn-SBAV versus 19.42% of the $MgMn_{1.88}Al_{0.13}O_4$ phase with tetragonal symmetry and 80.52% of the $MgMn_{1.75}Al_{0.25}O_4$ phase which has cubic symmetry. The dominant phase for Mn-SBAV900 is $MgAl_2O_4$ with cubic symmetry and total phase concentration equal

to 97.69%, versus only 1.86% of the $MgMn_{1.75}Al_{0.25}O_4$ phase and 0.48% of the $MgMn_{1.88}Al_{0.13}O_4$ phase both with cubic and tetragonal symmetry, respectively.

The crystallographic behavior observed in the data suggests that the cubic phase tends to form in greater quantity because it presents greater structural stability compared to the tetragonal phase (Callister, 2007) and which is present in standard magnesium aluminate under all synthesis conditions.

Table 2 shows the summary of the phase percentages and their symmetries for the synthesized powders.

Figure 5. Phase concentration of pure $MgAl_2O_4$ and doped Mn samples at sites A and B.

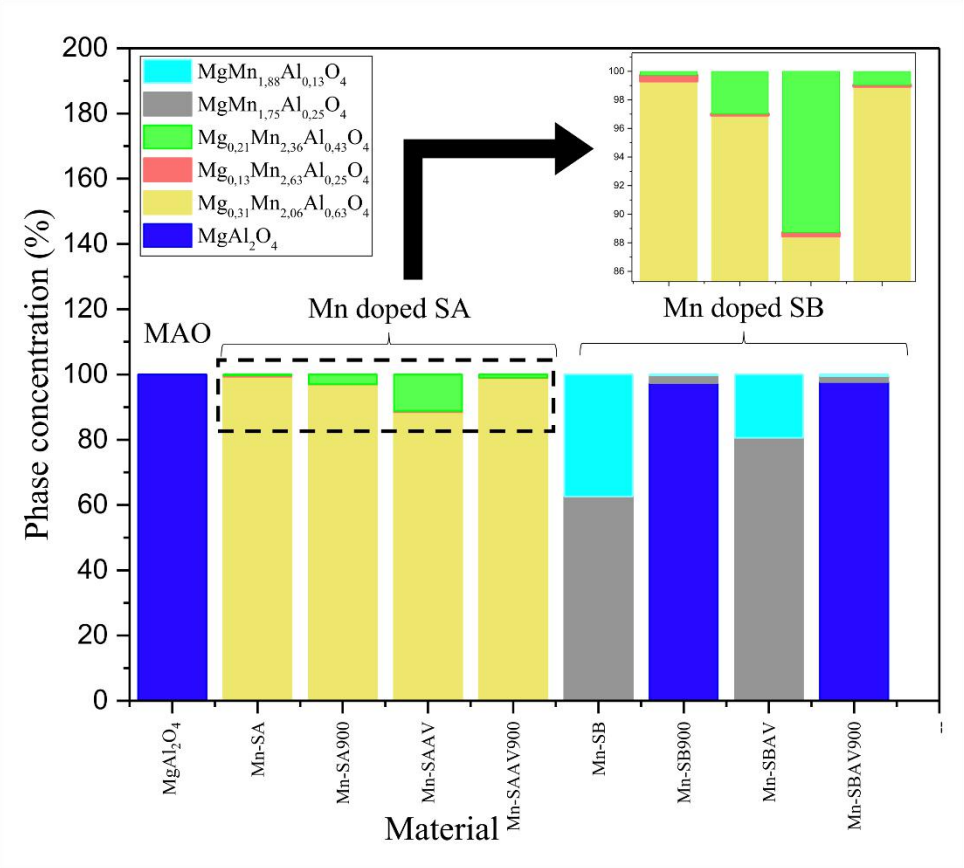

Source: Research data (Ferreira et al., 2022).

Table 2. Phase percentages and their symmetries for synthesized powders.

Material	Phase	Symmetry	Phase percentage (%)
MAO	$MgAl_2O_4$	Cubic	100
MAO900	$MgAl_2O_4$	Cubic	100
MAOAV	$MgAl_2O_4$	Cubic	100
MAOAV900	$MgAl_2O_4$	Cubic	100
Mn-SA	$Mg_{0.21}Mn_{2.36}Al_{0.43}O_4$	Tetragonal	0.27
	$Mg_{0.13}Mn_{2.63}Al_{0.25}O_4$	Tetragonal	0.40
	$Mg_{0.31}Mn_{2.06}Al_{0.63}O_4$	Cubic	99.32
Mn-SA900	$Mg_{0.21}Mn_{2.36}Al_{0.43}O_4$	Tetragonal	2.97
	$Mg_{0.13}Mn_{2.63}Al_{0.25}O_4$	Tetragonal	0.09
	$Mg_{0.31}Mn_{2.06}Al_{0.63}O_4$	Cubic	96.93
Mn-SAAV	$Mg_{0.21}Mn_{2.36}Al_{0.43}O_4$	Tetragonal	11.28
	$Mg_{0.13}Mn_{2.63}Al_{0.25}O_4$	Tetragonal	0.25
	$Mg_{0.31}Mn_{2.06}Al_{0.63}O_4$	Cubic	88.47
Mn-SAAV900	$Mg_{0.21}Mn_{2.36}Al_{0.43}O_4$	Tetragonal	0.96
	$Mg_{0.13}Mn_{2.63}Al_{0.25}O_4$	Tetragonal	0.08
	$Mg_{0.31}Mn_{2.06}Al_{0.63}O_4$	Cubic	98.95
Mn-SB	$MgMn_{1.88}Al_{0.13}O_4$	Tetragonal	37.39
	$MgMn_{1.75}Al_{0.25}O_4$	Cubic	62.61
Mn-SB900	$MgAl_2O_4$	Cubic	97.41
	$MgMn_{1.88}Al_{0.13}O_4$	Tetragonal	0.26
	$MgMn_{1.75}Al_{0.25}O_4$	Cubic	2.33
Mn-SBAV	$MgAl_2O_4$	Cubic	0.06
	$MgMn_{1.88}Al_{0.13}O_4$	Tetragonal	19.42
	$MgMn_{1.75}Al_{0.25}O_4$	Cubic	80.52
Mn-SBAV900	$MgAl_2O_4$	Cubic	97.69
	$MgMn_{1.88}Al_{0.13}O_4$	Tetragonal	0.48
	$MgMn_{1.75}Al_{0.25}O_4$	Cubic	1.86

Source: Research data (Ferreira et al., 2022).

4. Conclusion

Magnesium aluminates ($MgAl_2O_4$) with Mn substituting sites A and B were successfully synthesized by the microwave-assisted combustion method using Aloe Vera as a green chelating agent. The X-ray diffractometer (XRD) results generated through the crystallographic profiles showed that Aloe Vera was efficient in forming spinels in their pure states, and substituted by the manganese ion, showing that the adopted synthesis route is environmentally friendly. Although the plant extract has chelated biomolecules in the structure that change the crystallite size of the synthesized supports, the applied calcination increased the crystallinity of the materials, as well as the crystallite size in all scenarios due to the biomolecules being gasified. However, there was a greater difference in crystallinity for the supports substituted with manganese ion in site B due to the structural preference of the manganese ion for tetragonal symmetry.

The crystallite size decreased with the heat treatment, except for magnesium aluminates doped at site B due to the appearance of new phases that decrease the crystallite size.

Substituting the manganese ion at site A of the magnesium aluminate structure caused the formation of the following phases: $Mg_{0.21}Mn_{2.36}Al_{0.43}O_4$, $Mg_{0.13}Mn_{2.63}Al_{0.25}O_4$ and $Mg_{0.31}Mn_{2.06}Al_{0.63}O_4$. However, the following phases were formed for the substitution of the same ion in site B of $MgAl_2O_4$: $MgMn_{1.88}Al_{0.13}O4$ e $MgMn_{1.75}Al_{0.25}O_4$, in addition to the presence in a higher phase percentage of pure magnesium aluminate.

Acknowledgements

This study was partially financed by the Coordination for the Improvement of Higher Education Personnel - Brazil

(*CAPES*) – financing code 001. The authors thank *Capes* for the financial support, and the entire team of the Environmental Technology Laboratory (*LABTAM*) for their support in carrying out this study.

Referências

Alam, M. W., Kumar, V. G. D., Ravikumar, C. R., Prashantha, S. C., Murthy, H. C. A., & Kumar, M. R. A. (2021). Chromium (III) doped polycrystalline MgAl2O4 nanoparticles for photocatalytic and supercapacitor applications. *Journal of Physics and Chemistry of Solids*, 110491. https://doi.org/https://doi.org/10.1016/j.jpcs.2021.110491

Alhaji, A., Taherian, M. H., Ghorbani, S., & Sharifnia, S. A. (2019). Development of synthesis and granulation process of MgAl2O4 powder for the fabrication of transparent ceramic. *Optical Materials*, *98*, 109440. https://doi.org/https://doi.org/10.1016/j.optmat.2019.109440

Alvar, E. N., Rezaei, M., & Alvar, H. N. (2010). Synthesis of mesoporous nanocrystalline MgAl2O4 spinel via surfactant assisted precipitation route. *Powder Technology*, *198*(2), 275–278. https://doi.org/10.1016/j.powtec.2009.11.019

Azimi, G., Leion, H., Mattisson, T., Rydén, M., Snijkers, F., & Lyngfelt, A. (2014). Mn–Fe Oxides with Support of MgAl2O4, CeO2, ZrO2 and Y2O3–ZrO2 for Chemical-Looping Combustion and Chemical-Looping with Oxygen Uncoupling. *Industrial & Engineering Chemistry Research*, *53*(25), 10358–10365. https://doi.org/10.1021/ie500994m

Baghbanzadeh, M., Carbone, L., Cozzoli, P. D., & Kappe, C. O. (2011). Microwave-assisted synthesis of colloidal inorganic nanocrystals. *Angewandte Chemie - International Edition*, *50*(48), 11312–11359. https://doi.org/10.1002/anie.201101274

Boroujerdnia, M., & Obeydavi, A. (2016). Synthesis and characterization of NiO/ MgAl2O4 nanocrystals with high surface area by modified sol-gel method. *Microporous and Mesoporous Materials*, *228*, 289–296. https://doi.org/10.1016/j.micromeso.2016.04.006

Callister, W. D. (2007). Ciência e Engenharia de Materiais - Uma introdução. In *Ciência e Engenharia de Materiais - Uma introdução*.

Carvalho, L. S., de Melo e Melo, V. R., Sobrinho, E. V., Ruiz, D., & de Araújo Meloa, D. M. (2018). Effect of urea excess on the properties of the MgAl2O4 obtained by microwave-assisted combustion. *Materials Research*, *21*(1), 1–11. https://doi.org/10.1590/1980-5373-MR-2017-0189

Chandrababu, P., Cheriyan, S., & Raghavan, R. (2020). Aloe vera leaf extract-assisted facile green synthesis of amorphous Fe2O3 for catalytic thermal decomposition of ammonium perchlorate. *Journal of Thermal Analysis and Calorimetry*, *139*(1), 89–99. https://doi.org/10.1007/s10973-019-08376-5

Chandran, S. P., Chaudhary, M., Pasricha, R., Ahmad, A., & Sastry, M. (2006). Synthesis of Gold Nanotriangles and Silver Nanoparticles Using Aloe vera Plant Extract. *Biotechnology Progress*, *22*(2), 577–583. https://doi.org/10.1021/bp0501423

Chen, Q. Y., Meng, C. M., Lu, T. C., Chang, X. H., Ji, G. F., Zhang, L., & Zhao, F. (2010). Enhancement of sintering ability of magnesium aluminate spinel (MgAl2O4) ceramic nanopowders by shock compression. *Powder Technology*, *200*(1), 91–95. https://doi.org/https://doi.org/10.1016/j.powtec.2010.02.004

Chen, X. Y., Ma, C., Zhang, Z. J., & Li, X. X. (2009). Structure and photoluminescence study of porous red-emitting MgAl2O4:Eu3+ phosphor. *Microporous and Mesoporous Materials*, *123*(1), 202–208. https://doi.org/https://doi.org/10.1016/j.micromeso.2009.04.002

Chopade, S. C., Kore, I. G., Patil, S. P., Jadhav, N. D., Srinidhi, C., & Desai, P. A. (2018). Lattice geometry controlled synthesis of Cu – Doped nickel oxide nanoparticles. *Ceramics International*, *44*(5), 5621–5628. https://doi.org/https://doi.org/10.1016/j.ceramint.2017.12.209

Ewais, E. M. M., El-Amir, A. A. M., Besisa, D. H. A., Esmat, M., & El-Anadouli, B. E. H. (2017). Synthesis of nanocrystalline MgO/MgAl2O4 spinel powders from industrial wastes. *Journal of Alloys and Compounds*, *691*, 822–833. https://doi.org/https://doi.org/10.1016/j.jallcom.2016.08.279

Figueredo, G. P. de, Carvalho, A. F. M. de, Medeiros, R. L. B. de A., Silva, F. M., Macêdo, H. P. de, Melo, M. A. de F., & Melo, D. M. de A. (2017). Synthesis of MgAl2O4 by Gelatin Method: Effect of Temperature and Time of Calcination in Crystalline Structure. *Materials Research*, *20*(suppl 2), 254–259. https://doi.org/10.1590/1980-5373-mr-2017-0105

Ganesh, I. (2013). A review on magnesium aluminate (MgAl2O4) spinel: Synthesis, processing and applications. *International Materials Reviews*, *58*(2), 63–112. https://doi.org/10.1179/1743280412Y.0000000001

Ganesh, I., Johnson, R., Rao, G. V. N., Mahajan, Y. R., Madavendra, S. S., & Reddy, B. M. (2005). Microwave-assisted combustion synthesis of nanocrystalline MgAl 2O4 spinel powder. *Ceramics International*, *31*(1), 67–74. https://doi.org/10.1016/j.ceramint.2004.03.036

Golyeva, E. V., Kolesnikov, I. E., Lähderanta, E., Kurochkin, A. V., & Mikhailov, M. D. (2018). Effect of synthesis conditions on structural, morphological and luminescence properties of MgAl2O4:Eu3+ nanopowders. *Journal of Luminescence*, *194*(August 2017), 387–393. https://doi.org/10.1016/j.jlumin.2017.10.068

Golyeva, E. V., Vaishlia, E. I., Kurochkin, M. A., Kolesnikov, E. Y., Lähderanta, E., Semencha, A. V., & Kolesnikov, I. E. (2020). Nd3+ concentration effect on luminescent properties of MgAl2O4 nanopowders synthesized by modified Pechini method. *Journal of Solid State Chemistry*, *289*(May), 3–7. https://doi.org/10.1016/j.jssc.2020.121486

Govindarajan, D., & Roy, D. (2020). *Propane Dehydrogenation over Pt-Sn Supported on Magnesium Aluminate Material*. *14*(1), 37–44.

Grindlay, D., & Reynolds, T. (1986). The Aloe vera phenomenon: A review of the properties and modern uses of the leaf parenchyma gel. *Journal of Ethnopharmacology*, *16*(2), 117–151. https://doi.org/https://doi.org/10.1016/0378-8741(86)90085-1

Guo, J., Lou, H., Zhao, H., Chai, D., & Zheng, X. (2004). Dry reforming of methane over nickel catalysts supported on magnesium aluminate spinels. *Applied Catalysis A: General*, *273*(1–2), 75–82. https://doi.org/10.1016/j.apcata.2004.06.014

Hao, Y., Zhang, Y., & Wang, S. (2021). Synthesis, structure and photoluminescence of sheet-like MgAl2O4: Cr3+. *Inorganic Chemistry Communications*, *132*, 108853. https://doi.org/https://doi.org/10.1016/j.inoche.2021.108853

Jouini, A., Sato, H., Yoshikawa, A., Fukuda, T., Boulon, G., Kato, K., & Hanamura, E. (2006). Crystal growth and optical absorption of pure and Ti, Mn-doped MgAl2O4 spinel. *Journal of Crystal Growth*, *287*(2), 313–317. https://doi.org/https://doi.org/10.1016/j.jcrysgro.2005.11.027

Jung, K. W., Lee, S. Y., & Lee, Y. J. (2018). Facile one-pot hydrothermal synthesis of cubic spinel-type manganese ferrite/biochar composites for environmental remediation of heavy metals from aqueous solutions. *Bioresource Technology*, *261*(February), 1–9. https://doi.org/10.1016/j.biortech.2018.04.003

Katheria, S., Deo, G., & Kunzru, D. (2019). Rh-Ni/MgAl2O4 catalyst for steam reforming of methane: Effect of Rh doping, calcination temperature and its application on metal monoliths. *Applied Catalysis A: General*, *570*, 308–318. https://doi.org/https://doi.org/10.1016/j.apcata.2018.11.021

Khorramirad, M. M., Rahimipour, M. R., Hadavi, S. M. M., & Jozdani, K. S. (2018). The effect of magnesium compounds (MgO and MgAl2O4) on the synthesis of Lanthanum magnesium hexaaluminate (LaMgAl11O19) by solid-state reaction method. *Ceramics International*, *44*(5), 4734–4739. https://doi.org/10.1016/j.ceramint.2017.12.056

Kumar, S., Yadav, A., Yadav, M., & Yadav, J. P. (2017). Effect of climate change on phytochemical diversity, total phenolic content and in vitro antioxidant activity of Aloe vera (L.) Burm.f. *BMC Research Notes*, *10*(1), 60. https://doi.org/10.1186/s13104-017-2385-3

LAOKULa, P., KLINKAEWNARONGa, J., Phokha, S., & Seraphin, S. (2008). Indium oxide (In2O3) nanoparticles using Aloe vera plant extract: Synthesis and optical properties. *Optoelectronics and Advanced Materials, Rapid Communications*, *2*.

Li, G., Sun, Z., Chen, C., Cui, X., & Ren, R. (2007). Synthesis of nanocrystalline MgAl2O4 spinel powders by a novel chemical method. *Materials Letters*, *61*(17), 3585–3588. https://doi.org/https://doi.org/10.1016/j.matlet.2006.11.123

Li, R., Liu, J., Xu, L., & Zhou, J. (2020). Microwave idrothermal synthesis of magnesium-aluminium spinel. *Ceramics International*, *46*(18), 29207–29211. https://doi.org/10.1016/j.ceramint.2020.08.094

Liu, C., Lu, Y., Peng, Q., Xu, C., Yang, K., Li, X., Su, D., Li, Y., & Gao, F. (2021). The effect of Sr doping on the structural, mechanical, electronic properties and radiation tolerance of MgAl2O4 spinel: A first-principles study. *Journal of Alloys and Compounds*, *889*, 161614. https://doi.org/https://doi.org/10.1016/j.jallcom.2021.161614

Mahendiran, D., Subash, G., Arumai Selvan, D., Rehana, D., Senthil Kumar, R., & Kalilur Rahiman, A. (2017). Biosynthesis of Zinc Oxide Nanoparticles Using Plant Extracts of Aloe vera and Hibiscus sabdariffa: Phytochemical, Antibacterial, Antioxidant and Anti-proliferative Studies. *BioNanoScience*, *7*(3), 530–545. https://doi.org/10.1007/s12668-017-0418-y

MAUD - Materials Analysis Using Diffraction. (n.d.). Retrieved November 26, 2021, from http://www.ing.unitn.it/~maud/

Medeiros, R. L. B. A., Macedo, H. P., Oliveira, A. A. S., Melo, V. R. M., Carvalho, A. F. M., Melo, M. A. F., & Melo, D. M. A. (2016). Síntese de MgAl2O4 por combustão assistida por micro-ondas: influência dos parâmetros de síntese na formação e na estrutura cristalina. *Ceramica*, *62*(362), 191–197. https://doi.org/10.1590/0366-69132016623621961

Milani, S. S., Kakroudi, M. G., Vafa, N. P., Rahro, S., & Behboudi, F. (2021). Synthesis and characterization of MgAl2O4 spinel precursor sol prepared by inorganic salts. *Ceramics International*, *47*(4), 4813–4819. https://doi.org/https://doi.org/10.1016/j.ceramint.2020.10.051

Modanlou Juibari, N., & Eslami, A. (2019). Synthesis of nickel oxide nanorods by Aloe vera leaf extract. *Journal of Thermal Analysis and Calorimetry*, *136*(2), 913–923. https://doi.org/10.1007/s10973-018-7640-x

Nantharak, W., Wattanathana, W., Klysubun, W., Rimpongpisarn, T., Veranitisagul, C., Koonsaeng, N., & Laobuthee, A. (2017). Effect of local structure of Sm3+ in MgAl2O4:Sm3+ phosphors prepared by thermal decomposition of triethanolamine complexes on their luminescence property. *Journal of Alloys and Compounds*, *701*, 1019–1026. https://doi.org/https://doi.org/10.1016/j.jallcom.2017.01.090

Nascimento, R. A. B., Medeiros, R. L. B. A., Costa, T. R., Oliveira, Â. A. S., Macedo, H. P., Melo, M. A. F., & Melo, D. M. A. (2020). Mn/MgAl2O4 oxygen carriers for chemical looping combustion using coal: influence of the thermal treatment on the structure and reactivity. *Journal of Thermal Analysis and Calorimetry*, *140*(6), 2673–2685. https://doi.org/10.1007/s10973-019-09014-w

Nasrollahzadeh, M., Sajjadi, M., Dadashi, J., & Ghafuri, H. (2020). Pd-based nanoparticles: Plant-assisted biosynthesis, characterization, mechanism, stability, catalytic and antimicrobial activities. *Advances in Colloid and Interface Science*, *276*, 102103. https://doi.org/https://doi.org/10.1016/j.cis.2020.102103

Qiu, Z., Hao, H., Cao, M., Yao, Z., & Liu, H. (2018). Characteristics and structure of Mn-doped (0.6 − x)PMT–0.4PT–xPZ(x = 0.2,0.25) ternary system near morphotropic phase boundary. *Journal of Materials Science: Materials in Electronics*, *29*(16), 14261–14266. https://doi.org/10.1007/s10854-018-9559-1

R H Davis, M G Leitner, J. M. R. (1988). Aloe vera. A natural approach for treating wounds, edema, and pain in diabetes. *Journal of the American Podiatric Medical Association*, *78*(2), 60–68. https://doi.org/10.7547/87507315-78-2-60

Ragupathi, C., Vijaya, J. J., Surendhar, P., & Kennedy, L. J. (2014). Comparative investigation of nickel aluminate (NiAl2O4) nano and microstructures for the structural, optical and catalytic properties. *Polyhedron*, *72*, 1–7. https://doi.org/https://doi.org/10.1016/j.poly.2014.01.013

Rahmat, N., Yaakob, Z., Pudukudy, M., Rahman, N. A., & Jahaya, S. S. (2018). Single step solid-state fusion for MgAl2O4 spinel synthesis and its influence on the structural and textural properties. *Powder Technology*, *329*, 409–419. https://doi.org/10.1016/j.powtec.2018.02.007

Rasli, N. I., Basri, H., & Harun, Z. (2020). Zinc oxide from aloe vera extract: two-level factorial screening of biosynthesis parameters. *Heliyon*, *6*(1), e03156. https://doi.org/https://doi.org/10.1016/j.heliyon.2020.e03156

Reynolds, T., & Dweck, A. C. (1999). Aloe vera leaf gel: a review update. *Journal of Ethnopharmacology*, *68*(1), 3–37. https://doi.org/https://doi.org/10.1016/S0378-8741(99)00085-9

Routray, K. L., Saha, S., & Behera, D. (2019). Green synthesis approach for nano sized CoFe2O4 through aloe vera mediated sol-gel auto combustion method for high frequency devices. *Materials Chemistry and Physics*, *224*, 29–35. https://doi.org/https://doi.org/10.1016/j.matchemphys.2018.11.073

Saha, S., Das, S., Ghorai, U. K., Mazumder, N., Gupta, B. K., & Chattopadhyay, K. K. (2013). Charge compensation assisted enhanced photoluminescence derived from Li-codoped MgAl2O4:Eu3+ nanophosphors for solid state lighting applications. *Journal of the Chemical Society. Dalton Transactions*, *42*(36), 12965–12974. https://doi.org/10.1039/C3DT51411K

Sakuma, T., Minowa, S., Katsumata, T., Komuro, S., & Aizawa, H. (2014). Compositional variation of photoluminescence from Mn doped MgAl2O4 spinel. *Optical Materials*, *37*, 302–305. https://doi.org/https://doi.org/10.1016/j.optmat.2014.06.014

Sánchez, M., González-Burgos, E., Iglesias, I., & Gómez-Serranillos, M. P. (2020). Pharmacological Update Properties of Aloe Vera and its Major Active Constituents. *Molecules*, *25*(6), 1324. https://doi.org/10.3390/molecules25061324

Sangeetha, G., Rajeshwari, S., & Venckatesh, R. (2011). Green synthesis of zinc oxide nanoparticles by aloe barbadensis miller leaf extract: Structure and optical properties. *Materials Research Bulletin*, *46*(12), 2560–2566. https://doi.org/https://doi.org/10.1016/j.materresbull.2011.07.046

Sanjabi, S., & Obeydavi, A. (2015). Synthesis and characterization of nanocrystalline MgAl2O4 spinel via modified sol-gel method. *Journal of Alloys and Compounds*, *645*, 535–540. https://doi.org/10.1016/j.jallcom.2015.05.107

Selvarajan, E., & Mohanasrinivasan, V. (2013). Biosynthesis and characterization of ZnO nanoparticles using Lactobacillus plantarum VITES07. *Materials Letters*, *112*, 180–182. https://doi.org/https://doi.org/10.1016/j.matlet.2013.09.020

Shahid, F., Ismail, B., Khan, A. M., Ain, Q. U., Khan, R. A., Shah, F., Fazal, T., & Asghar, M. N. (2020). Cost effective way of tuning physical properties of MgAl2O4 spinel nanomaterials by Sr+2/ Mn2+ cations doped at the T-Sites. *Ceramics International*, *46*(8, Part A), 10710–10717. https://doi.org/https://doi.org/10.1016/j.ceramint.2020.01.078

Silva, T. H. S., Lima, C. G. M., Dutra, R. P. S., Aquino, F. de M., Grilo, J. P. F., Rajesh, S., & Macedo, D. A. (2017). Efeitos da dopagem com gadolínia na densificação e nas propriedades elétricas de soluções sólidas Ce0,99-xGdxCu0,01O2-δ. *Cerâmica*, *63*(368), 470–477. https://doi.org/10.1590/0366-69132017633682141

Sturm, G. S. J., Stefanidis, G. D., Verweij, M. D., Van Gerven, T. D. T., & Stankiewicz, A. I. (2010). Design principles of microwave applicators for small-scale process equipment. *Chemical Engineering and Processing: Process Intensification*, *49*(9), 912–922. https://doi.org/10.1016/j.cep.2010.07.017

Sun, G. H., Zhang, Q. L., Luo, J. Q., Li, L. C., Deng, Z., & Zhang, R. G. (2021). The effect of annealing on spectral characteristics of the Ti doped MgAl2O4 crystal. *Journal of Luminescence*, *234*, 117956. https://doi.org/https://doi.org/10.1016/j.jlumin.2021.117956

Takebuchi, Y., Fukushima, H., Kato, T., Nakauchi, D., Kawaguchi, N., & Yanagida, T. (2020). Effect of Ti-doping on dosimetric properties of MgAl2O4 single crystals. *Radiation Physics and Chemistry*, *177*, 109163. https://doi.org/https://doi.org/10.1016/j.radphyschem.2020.109163

Thongam, D. D., & Chaturvedi, H. (2021). Effect of biochemical compounds on ZnO nanomaterial preparation using aloe vera and lemon extracts. *Materials Today: Proceedings*, *44*, 4299–4304. https://doi.org/https://doi.org/10.1016/j.matpr.2020.10.548

Venkateswarlu, S., & Yoon, M. (2015). Surfactant-Free Green Synthesis of Fe 3 O 4 Nanoparticles capped with 3,4-Dihydroxyphenethylcarbamodithioate: Stable Recyclable Magnetic Nanoparticles for Rapid and Efficient Removal of Hg(II) Ions from Water. *Dalton Transactions (Cambridge, England : 2003)*, *44*. https://doi.org/10.1039/c5dt03155a

Wenisch, C., Kurland, H.-D., Grabow, J., & Müller, F. A. (2016). Europium(III)-Doped MgAl2O4 Spinel Nanophosphor Prepared by CO2 Laser Co-Vaporization. *Journal of the American Ceramic Society*, *99*(8), 2561–2564. https://doi.org/https://doi.org/10.1111/jace.14383

Xiao, G., Liu, Q., Wang, S., Komvokis, V. G., Amiridis, M. D., Heyden, A., Ma, S., & Chen, F. (2012). Synthesis and characterization of Mo-doped SrFeO3−δ as cathode materials for solid oxide fuel cells. *Journal of Power Sources*, *202*, 63–69. https://doi.org/https://doi.org/10.1016/j.jpowsour.2011.11.021

Xie, Q., Miao, C., Hua, W., Yue, Y., & Gao, Z. (2021). Ga-Doped MgAl2O4 Spinel as an Efficient Catalyst for Ethane Dehydrogenation to Ethylene Assisted by CO2. *Industrial & Engineering Chemistry Research*, *60*(31), 11707–11714. https://doi.org/10.1021/acs.iecr.1c01641

Yıldırım, Ö. A., Unalan, H. E., & Durucan, C. (2013). Highly Efficient Room Temperature Synthesis of Silver-Doped Zinc Oxide (ZnO:Ag) Nanoparticles: Structural, Optical, and Photocatalytic Properties. *Journal of the American Ceramic Society*, *96*(3), 766–773. https://doi.org/https://doi.org/10.1111/jace.12218

Yousefi, S., Haghighi, M., & Rahmani Vahid, B. (2018). Facile and efficient microwave combustion fabrication of Mg-spinel as support for MgO nanocatalyst used in biodiesel production from sunflower oil: Fuel type approach. *Chemical Engineering Research and Design*, *138*, 506–518. https://doi.org/10.1016/j.cherd.2018.09.013

Yu, S., Hu, Y., Cui, H., Cheng, Z., & Zhou, Z. (2021). Ni-based catalysts supported on MgAl2O4 with different properties for combined steam and CO2 reforming of methane. *Chemical Engineering Science*, *232*, 116379. https://doi.org/https://doi.org/10.1016/j.ces.2020.116379